Evaluating performance and cycle life improvements in the latest generations of prismatic lithium-ion batteries

Pontus Svens [a, b, *], Jens Groot [c], Alexander Smith [a], Matthew J. Lacey [b], Rakel Wreland Lindström [a], Göran Lindbergh [a]

[a] Applied electrochemistry, KTH Royal Institute of Technology, SE-100 44 Stockholm, Sweden.
[b] Scania CV AB, SE-151 87 Södertälje, Sweden.
[c] VOLVO Car Corporation, SE-405 31 Göteborg, Sweden.

*Corresponding author.
E-mail address: ponsvens@kth.se

Abstract

The last decade has seen an enormous improvement of energy density for lithium-ion battery cells, particularly for automotive grade cells intended for use in electrified vehicles. This has led to vastly improved range for battery electric vehicles as well as for plug-in hybrids. However, the challenge of uncertain battery lifetime remains. The ageing effect due to fast charging is especially difficult to predict due to its non-linear dependence on charge rate, state-of-charge and temperature. We here present results from fast charging (1C and 3C in a 20 % to 80 % SOC-level) of several energy-optimized, prismatic lithium-ion battery cell generations utilizing NMC/graphite chemistry through comparison of capacity retention, resistance and dQ/dV analysis. Considerable improvements are observed throughout cell generations and the results imply that acceptable cycle life can be expected, even under fast charging, when restricting the usage of the available battery capacity. Even though this approach reduces the useable energy density of a battery system, this trade-off could still be acceptable for vehicle applications where conventional overnight charging is not possible. The tested cell format (the VDA PHEV2-standard) has been used for a decade in different electrified vehicles. The ongoing development and improvement of this cell format by several battery cell manufacturers suggests it will continue to be a good choice for future vehicles.

Keywords: Fast charging; Lithium-ion battery; Ageing; PHEV2 battery cells; Electric vehicle

Introduction

Electrified vehicles such as hybrid electric vehicles (HEV), plug-in hybrid electric vehicles (PHEV), battery electric vehicles (BEV) and fuel cell electric vehicles (FCEV) are now established on the market. The powertrain technology has been proven for both passenger cars and commercial vehicles such as buses and trucks, despite relatively high component costs when compared to conventional vehicles. Despite very rapid development in terms increasing energy density and decreasing cell cost, the battery remains the critical component in EVs when evaluating total cost, service life and performance. Li-ion battery cells experience ageing, i.e. loss of capacity and power, during both storage (calendar ageing) and usage (cycle ageing) due to several ageing mechanisms for which the individual reaction rates depend strongly on operating conditions such as temperature, charge level (state-of-charge, SOC), charge/discharge currents and load cycle characteristics. In addition, many of the ageing mechanisms are inter-dependent. The charge rate can in many cases be regarded as the dominant ageing factor, especially for energy-optimized cells cycled within large state-of-charge (SOC) windows, as are typical for EVs and PHEVs. At the same time, fast-charging capability is widely desired for both passenger cars and commercial vehicles. Subsequently, the vehicle industry needs to develop accurate ageing models to develop robust battery systems and to forecast actual service life for the batteries.

The Swedish automotive industry and several universities have, within continuous research collaboration, carried out a number of studies on ageing of automotive grade Li-ion battery cells, through cycling and post-mortem analysis. In the first phase, focused on LFP/Graphite battery cells, it was shown that ageing may be severely non-uniformly distributed within the battery cells, especially for those that have been exposed to high charge rates. This distribution was observed both laterally across the jelly roll surface [1] and throughout the depth of the electrodes [2]. In this cell type, the graphite electrode was particularly affected by severe ageing. [1, 2]. The uneven ageing was argued to be a consequence of inhomogeneous current distribution due to the tab positions, as well as internal variations in temperature, electrolyte wetting and pressure. In the second phase of the research collaboration, the ageing effects of fast charging on NMC111/Graphite cells were studied. From careful post-mortem analysis it could be concluded that different ageing mechanisms dominate, depending on the charging rate [3]. While NMC particle cracking was observed at 1-2C charging rate, lithium plating likely reduced lifetime at 3C charging rate, and gas evolution rapidly killed the cells cycled with 4C charging rate. In a separate study of a similar cell [4], it was observed by on-line mass spectrometry that the high ageing rate under fast charging was associated with the evolution of large quantities of ethylene gas. Even for NMC111/graphite cells, heterogeneous ageing within the cell was observed. For instance, a difference in direct current internal resistance (DCIR) was observed among samples harvested from the curved and the flat regions of the prismatic cell jelly roll, pointing towards a nonuniform distribution of mechanical pressure affecting the local ageing [5]. The negative electrode is known to be a major bottleneck for practical fast charging rates (i.e. less than 1 hour charging for energy-optimized cells) [6]. This is mainly due to the slow kinetics of lithium insertion into graphite, the typical negative electrode material of choice for energy-optimized cells. If graphite particles are unable to intercalate lithium ions at sufficiently high rate, then lithium deposits onto the particles as tree-like, highly-reactive, metallic dendrites, a process referred to as lithium plating. These dendrites can grow through the separator and hence cause internal short-circuits in the cell or, in less severe cases, cause accelerated electrolyte degradation and subsequent loss of cyclable lithium and increase of cell resistance.

In the past, large-format cells have been seldom studied, probably due to the high cost and scarce availability of this type of automotive grade cells. In this work however, we compare performance and ageing for several generations of automotive grade cells. Results are summarized from cycle ageing of

three different NMC111/graphite cells performed within this research consortium over the course of several years. The comparisons herein emphasize the progress between the different generations of energy optimized cells. The capacity retention curves after cycling under 1C and 3C charge (which correspond to fully charging the battery in 60 and 20 minutes, respectively) are compared, as well as corresponding DCIR and dQ/dV analyses. Finally, we discuss the progress in performance and durability of this type of cells and include preliminary comparison with a nickel-rich NMC811/graphite cell type cycled within the present third phase of the collaboration.

Experimental

Three different types of prismatic battery cells of the VDA (Verband der Automobilindustrie) PHEV2 format (148 x 26.5 x 91 mm) [7] were cycled at the same temperature and in the same SOC-region. The electrode active material is NMC111/graphite for the three tested cell types. Cycling was done in a 20 % to 80 % SOC window, with constant current charge and discharge currents. The charge and discharge time required to stay in the SOC-window was recalculated every 200th cycle from periodically performed capacity measurements. In addition to the periodic capacity measurements, DCIR measurements were also performed, followed by constant voltage adjustment to 80 % SOC before the next cycling period. Two cells of each cell type were cycled at 1C/1C (charge/discharge) current and two cells per cell type at 3C/1C. One additional cell type, called D, in the same format but with the electrode active material NMC811/graphite is used as reference but was not included in the original test matrix. This cell type has been cycled under other conditions and detailed results from that work will be published separately. Additional information about all cell types is shown in Table 1.

Table 1 Summarized information about the cell types tested in this study

Cell type	Market introduction	Capacity (Ah)	Voltage range (V)	Max. rated charge
A	2012	25	3.00 – 4.10	1 C
B	2014	28	2.80 – 4.15	1 C
C	2016	37	3.00 – 4.20	1 C
D	2018	~50	3.00 – 4.20	~1.5 C

For the cell type C, reference cells were also stored in different temperatures during the testing period in order to measure the calendar ageing separately. The conditions for the cell cycling and reference performance testing of cell types A and B, which were cycled at the same test facility, are described in detail in previous work [3]. The cycling of cell type C was done at another test facility under the following conditions. Cycling and performance testing were done on a Maccor Series 4000 cell tester. All cells were placed in a climate chamber operating at an average temperature of +33 ± 1 °C during testing to obtain an average cell skin temperature of +35 °C (measured individually with surface-mounted thermocouples). Steel plates were attached to all cells during cycling to maintain external cell pressure according to supplier recommendation. The applied test protocol was the same as for cell types A and B.

Results

Capacity

The capacity fade behaviour of cell types A, B and C differs from each other in several ways. A clear difference in ageing characteristics is seen in the appearance of the capacity retention curves. Comparison of different slopes in the capacity retention curves can be done by fitting curves based on coulombic efficiency (CE) calculations. Coulombic efficiency has been used in earlier research as a tool for analysing ageing [8-10]. If a constant CE is assumed, the capacity retention can be estimated according to following equation:

$$Q = \eta^{Neq} \tag{1}$$

where Q is the capacity retention, η is the coulombic efficiency and N_{eq} is the corresponding number of equivalent full cycles. Using this approach, it is possible to identify three different CE-slopes for the capacity retention of cell type A at 1C charge current, as seen in Figure 1a. Also for cell type B, three different CE-slopes for the capacity retention are identified under 1C charging, depicted in Figure 1c. Both cell types experience an increasing coulombic efficiency under 1C charging, hence showing a regressive or decelerating aging behaviour beginning after a couple hundred equivalent full cycles. The capacity retention for cell type A can be fitted with a single CE-curve for the 3C charging case, as seen in Figure 1b. It can be noted that the estimated coulombic efficiency in this case is similar to the estimated CE1 for the 1C cycled cell type A in Figure 1a. A similar behaviour is also seen for cell type B under 3C charge; its fitted CE-curve also has an efficiency corresponding to the first fitted CE-curve for the 1C cycled cells. However, in this case there is also a sudden change in slope at around 80% remaining capacity, where the estimated coulombic efficiency decreases drastically (CE2 in Figure 1d). The capacity retention curves for cell type C are very similar to that of cell type B (Figure 1e and f), i.e. a decelerated ageing rate for the first few hundred cycles, followed by ageing at a constant CE-rate between 90 % and 80 % capacity retention. In addition, there are signs of accelerating ageing towards EOL for the cells cycled with the 3C charge strategy, where the overall lifetime is only about one third of that for the corresponding cells cycled with 1C charging.

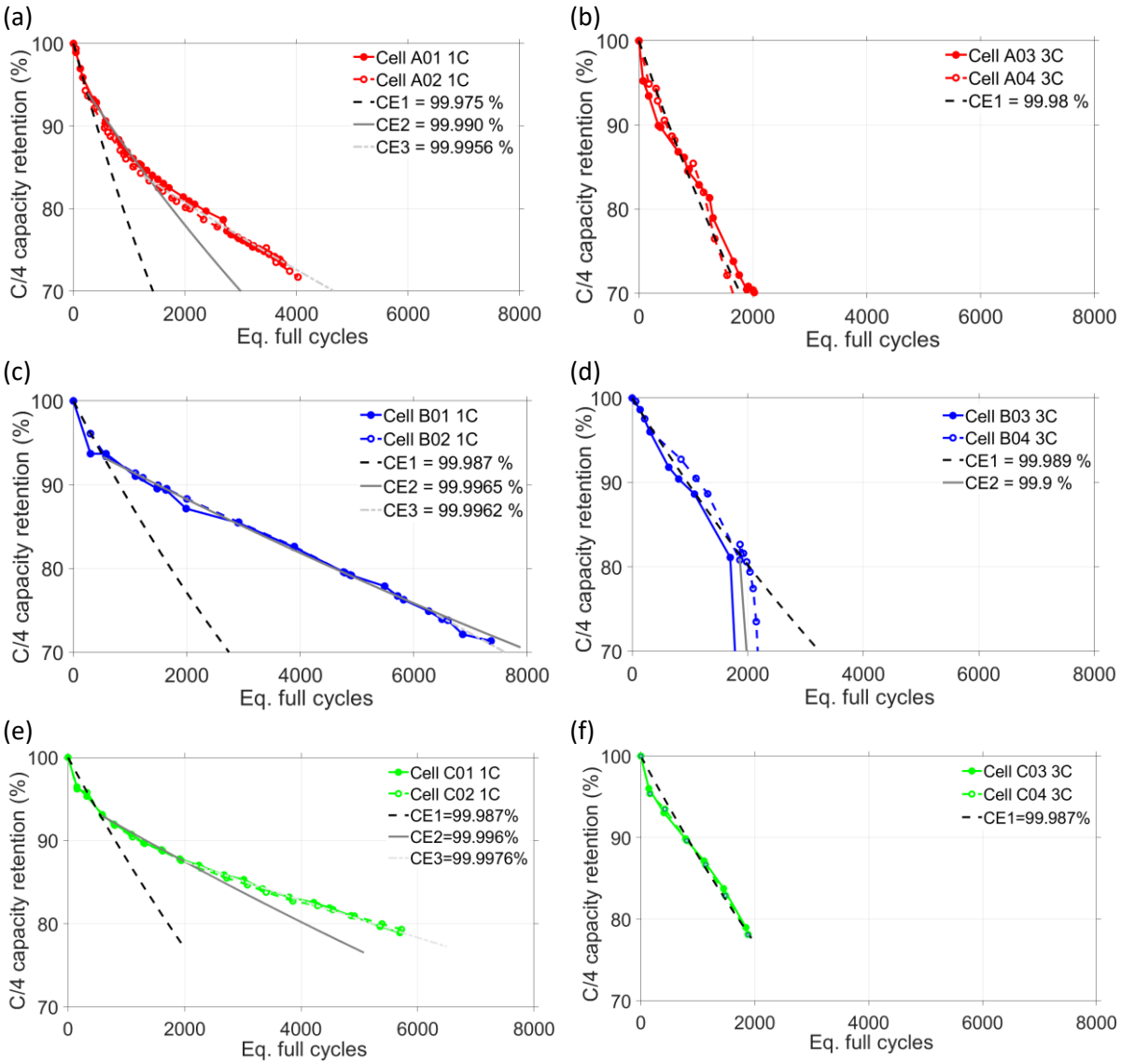

Figure 1 Capacity retention for ageing at 35 °C, including fitted constant coulombic efficiency curves for a) cell type A at 1C cycling, b) cell type A at 3C cycling, c) cell type B at 1C cycling, d) cell type B at 3C cycling, e) cell type C at 1C cycling and f) cell type C at 3C cycling

In summary, the results from the capacity fade analysis show three typical regimes: decelerated, constant and accelerated ageing, i.e. sudden fade close to end-of-life, which is in line with similar published work by Waldmann et al. [11]. Using CE measurements on cells at the beginning of cell life could hence in some cases be helpful to predict battery cell cycle life, but there are cases where this type of extrapolation could either overestimate or underestimate battery lifetime. Regarding the test cases in this study, CE measurements at the beginning of the test could have been useful for predicting ageing of the cells cycled with the 3C charging regime, but they would have underestimated lifetime for cells cycled with the 1C charging regime. The accuracy and relevance of these CE measurements are greatly affected by the temperature and charge rate of each test [12]. Such characterization at BOL would also be very limited in its ability to predict subsequent changes in CE in the different ageing regimes.

The effective lifetime of the cells can be discussed as their cyclability, or, the number of cycles to reach 80 % SOH. A general improvement in cyclability was observed through the three subsequent cell candidate generations, with cell type A having the lowest cyclability and cell type C having the highest.

However, cell type B seems to have the largest spread between tested cell pairs at 3C charging which could be related to cell manufacturing or slight variations in test conditions.

Common for all three cell types is that 3C charging rates result in lower cyclability relative to 1C charging rates. The largest difference can be seen for cell type C that only shows around one third of the cycle life at 3C charging compared to 1C charging. In addition, for cell type C, a time dependent aging mechanism was also measured by means of a calendar aging test at 50 % SOC from which the results are presented in Figure 2. All cycled cells also showed swelling at end of testing, especially cells cycled at high charge C-rates.

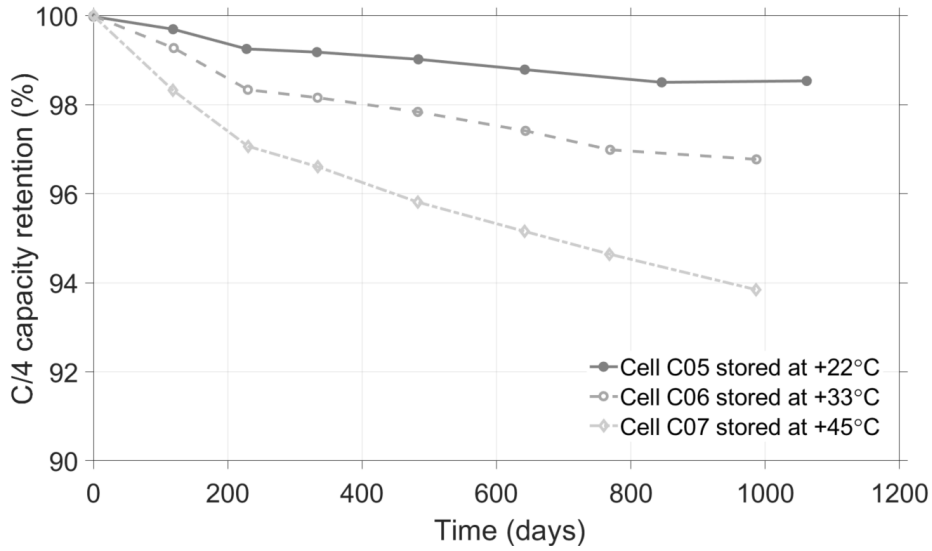

Figure 2 Calendar aging of cell type C stored at 50 % state-of-charge.

As expected, calendar ageing of this type of lithium-ion cell has a capacity loss dependency related to the square root of time [13, 14], with an Arrhenius temperature correction.

Direct current internal resistance

Direct current internal resistance (DCIR) was also measured on all cells throughout the testing. These measurements were done at a constant current pulse for short duration which captures information about electronic and ionic resistance of the cells. Cell type A has a steadily increasing DCIR throughout cycling, both for 1C and 3C charging, while cell types B and C reach an DCIR minimum after some hundred equivalent full cycles. This decrease in DCIR during early cycles is seldom reported in literature and could be related to several possible causes, of which one could be how the formation process differ between cell candidates [15]. Certain electrolyte additives or protective layers may also be used to stabilize the cell for storage before sale and use. The decrease may be related to the consumption of these sacrificial additives or some other activation behaviour inside the cell (e.g. porosity increase). As this minimum was not observed for the oldest cell type A, this likely reflects recent advances in cell materials, design, and production. For cell type A it hence seems possible to correlate capacity loss to DCIR rise with a linear fit under the conditions applied. However, it is seen from Figure 3 that despite this correlation, the spread between corresponding cells of cell type A is large. This makes estimation of remaining battery capacity from DCIR data challenging in a real-life vehicle application. The relationship between DCIR and capacity retention is not linear for cell types B and C. However, after the point where the cell DCIR reached the minimum, it could be possible to find a correlation between DCIR and capacity retention. This behaviour makes it considerably more complicated to apply a model for battery capacity estimation from DCIR measurements alone in a real-life vehicle application.

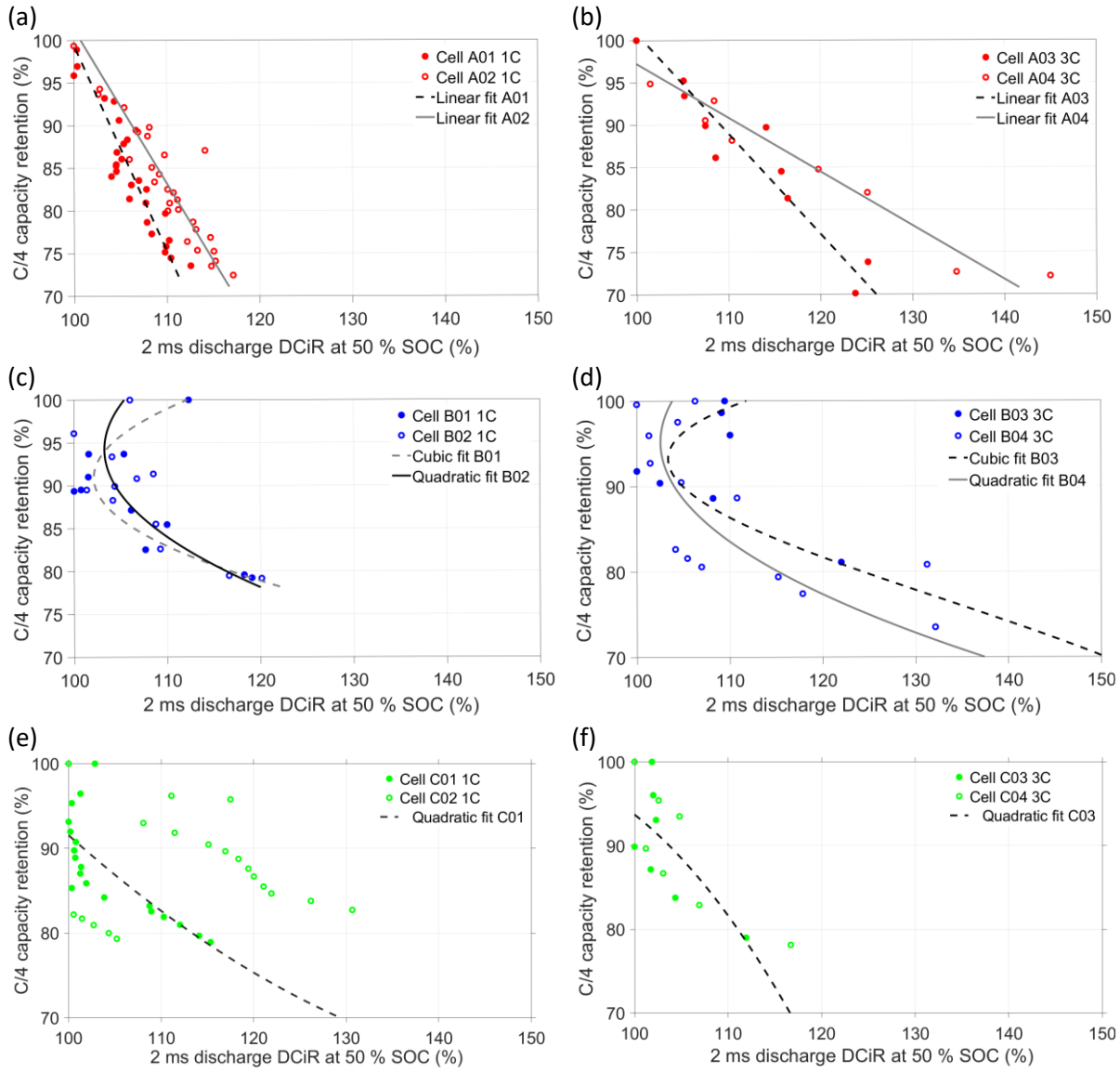

Figure 3 Graphical presentation of the correlation between DCIR and capacity retention for cell type A: a) 1C charged cells, b) 3C charged cells; for cell type B: c) 1C charged cells, d) 3C charged cells; and for cell type C: e), 1C charged cells, f) 3C charged cells

Qualitative capacity loss analysis

Incremental capacity analysis, i.e. analysing the inverse derivative (dQ/dV) of charge and discharge voltage curves versus voltage, has been demonstrated as a valuable tool to analyse ageing of the negative and positive electrode respectively [16]. This method was applied to all test cases and is presented for beginning of life and end of life in Figure 4. Peaks in dQ/dV curves relate to phase equilibrium of active electrode material (voltage plateaus in voltage versus capacity plots) [17]. For the cell type NMC111/graphite, two peaks are dominant, one at around 3.5 V mostly related to the negative active electrode material graphite and one at around 3.65 V mostly related to the positive active electrode material NMC111. For the 1C cycled type A cells depicted in Figure 4a, the low-voltage peak has moved to higher cell voltage at EOL, indicating loss of cyclable lithium [10, 16, 18, 19] However, the behaviour of the peak at 3.65 V is quite complicated, and could be linked to several different ageing phenomena. The loss of peak area could be related to a loss of NMC active material, though cursory analysis of the corresponding dV/dQ curves shows no strong

evidence for this. The decrease and shift in this 3.65 V peak is likely due primarily to the loss of cyclable lithium.

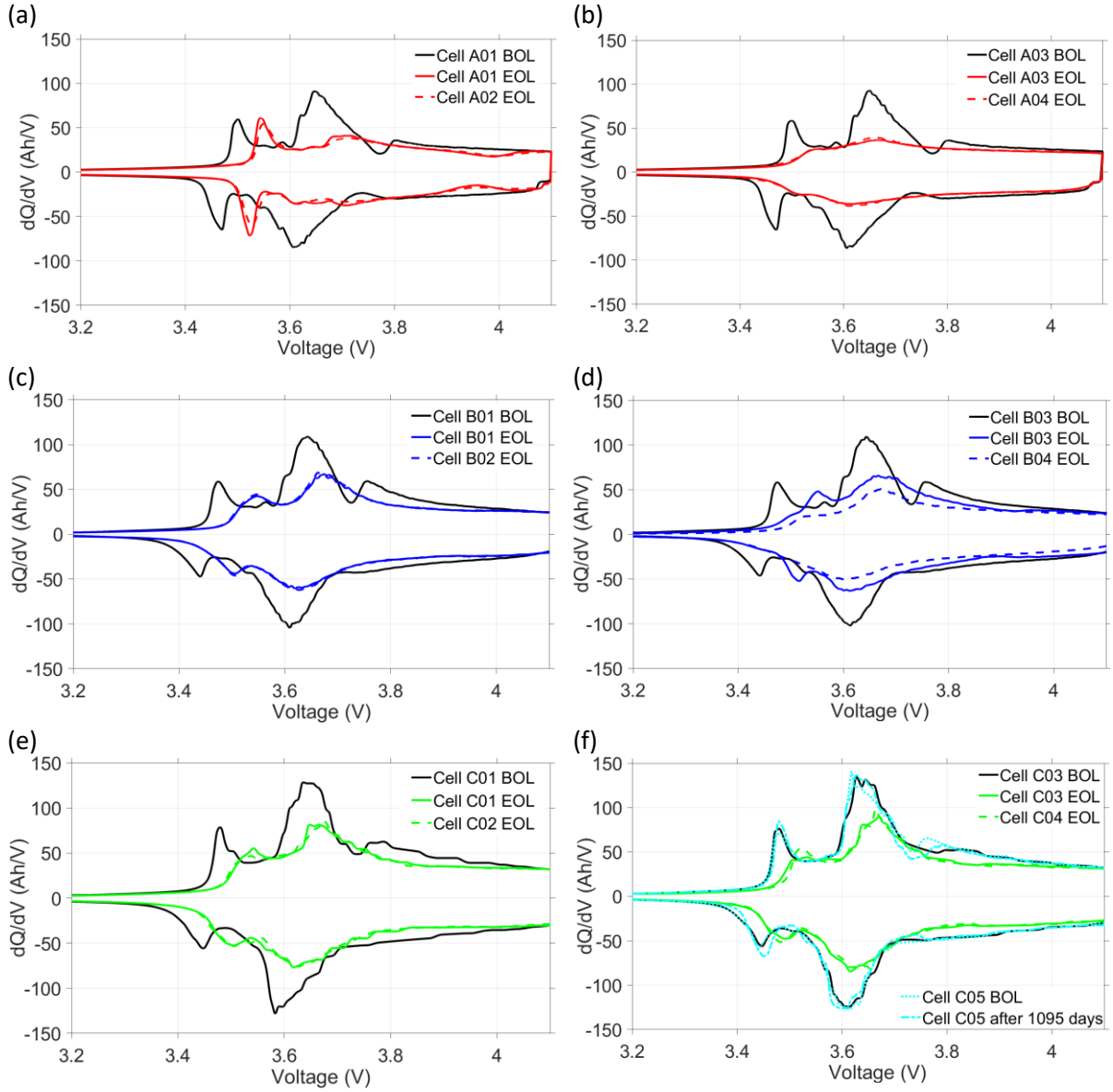

Figure 4 dQ/dV-plots for a) cell type A at 1C charge, b) cell type A at 3C charge, c) cell type B at 1C charge, d) cell type B at 3C charge, e) cell type C at 1C charge and f) cell type C at 3C charge and calendar aged (red curves)

On the other hand, for the 3C cycled type A cells depicted in Figure 4b, both main peak features have more or less disappeared at EOL. This could again indicate several different ageing phenomena or a combination thereof. Capacity attributed to the solid solution behaviour of NMC111 at cell voltages above 3.7 V appears to be retained [16, 20]. This capacity is observed as a constant, non-zero dQ/dV value at high voltage. This implies that while much of the positive electrode material remains intact, it may be incompletely lithiated on discharge due to limitations of the negative electrode, lithium inventory, or other factors. The marked decrease in the low-voltage peak further suggests that loss of graphite active material at the negative electrode may be responsible, alongside loss of cyclable lithium.

The behaviour of cell type B is depicted in Figure 4c and d. In this case, it is seen that both 1C and 3C cycled cells experience loss of area under both main peaks at EOL. Many of the peak features are better preserved under 3C cycling, indicating better rate capability compared to cell type A. Again, there appeared only slight losses at high voltage, indicating that loss of NMC performance may not be caused by loss of active material. Peak shifts indicating loss of cyclable lithium are observed, alongside a broadening of several peaks, particularly for the negative electrode. The sharp, well-defined peaks at BOL represent the electrochemical reactions in relatively homogenous electrodes. The broadening and smudging of these peaks at EOL indicate the occurrence of these reactions over wider windows of cell voltage. In this way, peak broadening indicates increasing heterogeneity and local gradients of both SOC and overpotential within the cell. Broadening without loss of integrated peak area does not entail loss of capacity.

Lastly, cell type C is depicted in Figure 4e and f. As with cell type B, features are not eliminated under 3C cycling, indicating acceptable rate capability. Broadening indicative of electrode heterogeneity is seen, but it is difficult to assess the relative impacts of loss of active material at each electrode. Both 1C and 3C cycled cases continue to show shift of the peaks indicating loss of cyclable lithium.

Discussion and summary

The energy density of prismatic lithium-ion battery cells of the PHEV2 VDA-format has increased significantly from the market introduction until the present. Our results on cell aging for NMC111/graphite PHEV2-size cells show that the evolution towards higher energy density is accompanied by an increased slow charging (1C) cyclability, while the fast (3C) charging cyclability has a much lower increase throughout cell generations (in a 20 % to 80 % SOC-window, Fig. 5). Regarding DCIR, the linear relationship between capacity retention and DCIR rise seen for the early version of this cell size has evolved to a more complex non-monotonic relationship. This may be a consequence of additives used to enhance shelf stability or cell performance. In any case, the increased complexity of DCIR data reveals an increasingly complex field of electrochemical phenomena within the cell and increases the difficulty of meaningful cell monitoring.

Both early and more recent versions of the PHEV2-format cells show tendencies of swelling towards EOL, especially at higher (3C) charging currents. Such swelling can be due to expansion of the solid-phase electrode materials as well as gas generation from breakdown of the liquid electrolyte.

Cell type A shows more severe aging of the NMC111 material compared to graphite when cycled at slower charging currents. However, the graphite seems to be more affected by cycling at higher charging currents. When compared to cell types B and C, which in turn show no severe loss of active material, it appears that optimizations have been implemented to improve the performance and longevity of the NMC and graphite electrodes. All three cell types also show loss of cyclable lithium upon cycling, both at slow and fast charging currents. One possible explanation of the different aging behaviours between cell types could be that different rates of loss of cyclable lithium affect the final outcome of electrode active material loss at EOL [21]. In some cases, loss of cyclable lithium by formation of a solid-electrolyte interphase could help to passivate certain mechanisms and hold particles together. However, after a certain amount lost, local overpotentials could increase to the point that lithium plating [22]or other catastrophic mechanisms are induced. One such mechanism could be electrode dry out due to long-term

electrolyte degradation [3, 10]. In this way, the internal electrochemical environment is dynamic and changing with age of the cell.

These changing mechanisms of passivation and aging could contribute to fitted changes in coulombic efficiency during the life of a cell. For each cell type, the initial coulombic efficiency appears to be similar for both slow charging and fast charging. When cycling with high charging currents, a constant coulombic efficiency is seen until EOL; in some cases there is a shift to sudden fade (decreased coulombic efficiency) close to EOL. When cycling with low charging currents, the initial low coulombic efficiency improves after a few hundred equivalent full cycles, sometimes in several steps. This decelerated ageing behaviour is well known for lithium-ion batteries but still hard to predict in models, especially if it is followed by a sudden fade.

Overall, our results indicate that this type of cell could be suitable for applications such as PHEV distribution trucks, where there are demands for zero tail pipe emissions and silent driving during night delivery. However, to obtain a reasonable lifetime from a corresponding battery pack, the charging rate should be limited to around 1C. For example, a PHEV distribution truck that cycles the battery between 20 % and 80 % SOC two times per day for 250 days per year should, in the best case, be able to achieve a battery service life of around 10 years (until 80 % capacity retention), as estimated from the data obtained for cell type C. With a 3C charging regime this figure would instead be less than 4 years, which could be challenging for the customer. For heavy-duty BEV applications where all traction and auxiliary energy needs to come from the battery, a traction battery with very high energy density is needed. In applications where charging can be done during longer periods (< 1C), a pure energy-optimized cell type should be a suitable choice. Today, more energy-optimized cells in the PHEV2-size are also available. For example, it has from around 2019 been possible to obtain PHEV2-size cells with around 50 Ah from selected cell suppliers [23]. These cells seem to utilize a nickel-rich NMC positive active electrode material, sometimes also in combination with a silicon-containing graphite negative active electrode to reach high capacity. Looking into the future, from a simple model based on current cell designs, we project that a high-nickel-content cathode combined with a solid-state electrolyte could push future PHEV2 battery cell capacities towards 100 Ah, corresponding to a very high energy density as well as specific energy (>350 Wh/kg, >1000 Wh/L). Since the trend in automotive electrification increasingly points towards pure BEVs, many battery suppliers are focusing on developing more energy-dense battery cells. This development over the course of cell types A (2012), B (2014), C (2016), and beyond is shown in Figure 5.

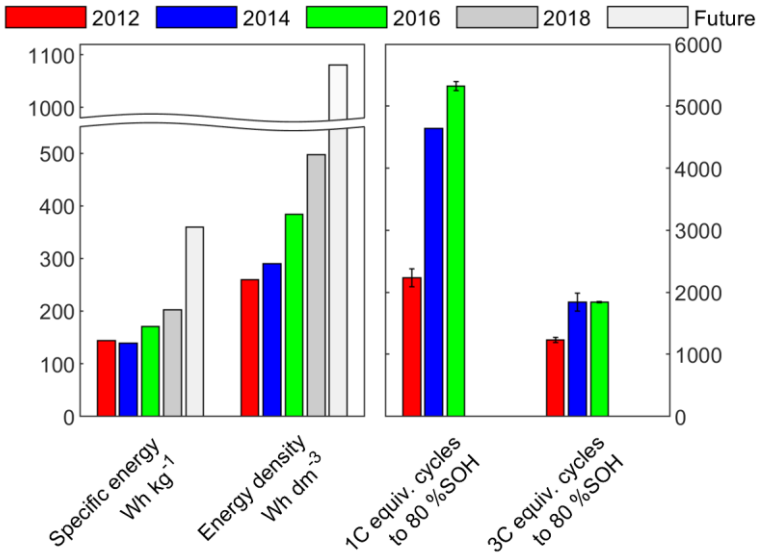

Figure 5 Comparison between the PHEV2-size cell generations regarding performance and capacity improvement, also considering the current PHEV2-cell versions available on the market and an outlook considering future chemistries.

In addition to the improvement in energy density throughout cell generations, there is also an improvement in specific energy, though this is less pronounced. This means that for each generation of cells in this format, more capacity can be fit into the same cell housing, but at a greater weight. This effective densification of the cells has interesting implications for the automotive industry. A battery pack built with a certain size specification in 2018 may deliver about 90 % more energy than a visually-identical pack built in 2012, but will also be around 30 % heavier, assuming a gravimetric cell-to-pack ratio of 60 %. Hence, the same weight of batteries would in 2018 have given a 38 % increase in capacity compared to 2012. The impact of this trade-off between pack energy and pack weight can be far-reaching for mobile applications. Trucks designed with heavier battery packs would in some cases have to sacrifice payload in favour of range. However, alongside these increases in energy density and specific energy, it can also be noted from Figure 5 that the cyclability using the 1C-charge strategy is vastly improved throughout the generations while cyclability using 3C-charge has had a slower rate of improvement.

Conclusions

We have compared three different lithium-ion battery cell generations of the prismatic VDA-standard PHEV2 regarding lifetime, with focus on the usage in electrified heavy-duty vehicles. The energy density has increased by almost 50 % over a four-year period and three cell generations, while the specific energy has increased by a more moderate 18 %. The equivalent full cycle throughput, under 1C/1C charge/discharge in a 20 % to 80 % SOC-window and at +35 °C, is also much improved through cell generations while a more moderate increase in cyclability at 3C/1C is seen. The DCIR behaviour changes throughout the cell generations from a linear relationship with capacity retention to a non-monotonic one. Present versions of the VDA PHEV2 cell format offer almost 50 Ah capacity, which means an impressively doubled capacity in 8 years. Altogether, the results from this study point out that the VDA PHEV2 cell format is still a viable choice for electrified heavy-duty vehicles such as inner-city distribution PHEV trucks or even BEVs.

Acknowledgement

This work was funded by the Swedish Environmental Protection Agency, the Swedish Energy Agency, the Swedish Electromobility Centre, the VOLVO Group and Scania CV AB, and the Swedish governmental initiative Stand-Up for Energy. The cycling was carried out within the *Batterifonden* project *Fast-Charging of Large Energy-optimized Li-ion Cells for Electrified Drivelines* (Grant number: P40501-1) and the *Energy Efficient Vehicles program* project *Electrochemical study of durability aspects in large vehicle batteries* (Grant number: 30770-1) and could be realized through the *Batterifonden* project *Ageing of Lithium-Ion battery cells with Nickel-rich Electrodes* (*ALINE*) (Grant number: 2017-013611). The authors would like to thank all industrial and academic participants from the consortium for contribution though out the various projects.

References

[1] M. Klett *et al.*, "Non-uniform aging of cycled commercial LiFePO4//graphite cylindrical cells revealed by post-mortem analysis," *Journal of Power Sources,* vol. 257, no. 0, pp. 126-137, 7/1/ 2014, doi: http://dx.doi.org/10.1016/j.jpowsour.2014.01.105.

[2] M. Klett *et al.*, "Uneven Film Formation across Depth of Porous Graphite Electrodes in Cycled Commercial Li-Ion Batteries," *The Journal of Physical Chemistry C,* vol. 119, no. 1, pp. 90-100, 2015/01/08 2015, doi: 10.1021/jp509665e.

[3] A. S. Mussa *et al.*, "Fast-charging effects on ageing for energy-optimized automotive LiNi1/3Mn1/3Co1/3O2/graphite prismatic lithium-ion cells," *Journal of Power Sources,* vol. 422, pp. 175-184, May 2019, doi: 10.1016/j.jpowsour.2019.02.095.

[4] U. Mattinen, M. Klett, G. Lindbergh, and R. W. Lindstrom, "Gas evolution in commercial Li-ion battery cells measured by on-line mass spectrometry - Effects of C-rate and cell voltage," *Journal of Power Sources,* vol. 477, Nov 2020, Art no. 228968, doi: 10.1016/j.jpowsour.2020.228968.

[5] A. S. Mussa, G. Lindbergh, M. Klett, P. Gudmundson, P. Svens, and R. W. Lindström, "Inhomogeneous active layer contact loss in a cycled prismatic lithium-ion cell caused by the jelly-roll curvature," *Journal of Energy Storage,* vol. 20, pp. 213-217, 2018.

[6] S. Ahmed *et al.*, "Enabling fast charging - A battery technology gap assessment," *Journal of Power Sources,* vol. 367, pp. 250-262, Nov 2017, doi: 10.1016/j.jpowsour.2017.06.055.

[7] *Industry Review of xEV Battery Size Standards*, B. C. S. S. Committee, 2018. [Online]. Available: https://doi.org/10.4271/J3124_201806

[8] A. J. Smith, J. C. Burns, S. Trussler, and J. R. Dahn, "Precision Measurements of the Coulombic Efficiency of Lithium-Ion Batteries and of Electrode Materials for Lithium-Ion Batteries," *Journal of The Electrochemical Society,* vol. 157, no. 2, pp. A196-A202, 2010, doi: 10.1149/1.3268129.

[9] A. J. Smith, J. C. Burns, D. Xiong, and J. R. Dahn, "Interpreting High Precision Coulometry Results on Li-ion Cells," *Journal of The Electrochemical Society,* vol. 158, no. 10, pp. A1136-A1142, 2011, doi: 10.1149/1.3625232.

[10] D. A. Stevens, R. Y. Ying, R. Fathi, J. N. Reimers, J. E. Harlow, and J. R. Dahn, "Using High Precision Coulometry Measurements to Compare the Degradation Mechanisms of NMC/LMO and NMC-Only Automotive Scale Pouch Cells," *Journal of the Electrochemical Society,* vol. 161, no. 9, pp. A1364-A1370, 2014 2014, doi: 10.1149/2.0971409jes.

[11] T. Waldmann, B.-I. Hogg, and M. Wohlfahrt-Mehrens, "Li plating as unwanted side reaction in commercial Li-ion cells–A review," *Journal of Power Sources,* vol. 384, pp. 107-124, 2018.

[12] J. C. Burns, D. A. Stevens, and J. R. Dahn, "In-Situ Detection of Lithium Plating Using High Precision Coulometry," *Journal of The Electrochemical Society,* vol. 162, no. 6, pp. A959-A964, 2015, doi: 10.1149/2.0621506jes.

[13] I. Bloom, L. K. Walker, J. K. Basco, D. P. Abraham, J. P. Christophersen, and C. D. Ho, "Differential voltage analyses of high-power lithium-ion cells. 4. Cells containing NMC," *Journal*

of Power Sources, vol. 195, no. 3, p. 877, 2010, doi: https://doi.org/10.1016/j.jpowsour.2009.08.019.

[14] A. J. Smith, J. C. Burns, X. Zhao, D. Xiong, and J. R. Dahn, "A high precision coulometry study of the SEI growth in Li/graphite cells," *Journal of The Electrochemical Society,* vol. 158, no. 5, pp. A447-A452, 2011, doi: 10.1149/1.3557892.

[15] T. S. Pathan, M. Rashid, M. Walker, W. D. Widanage, and E. Kendrick, "Active formation of Li-ion batteries and its effect on cycle life," *Journal of Physics: Energy,* vol. 1, no. 4, p. 044003, 2019/08/22 2019, doi: 10.1088/2515-7655/ab2e92.

[16] M. Dubarry, V. Svoboda, R. Hwu, and B. Y. Liaw, "Incremental capacity analysis and close-to-equilibrium OCV measurements to quantify capacity fade in commercial rechargeable lithium batteries," *Electrochemical and Solid State Letters,* vol. 9, no. 10, pp. A454-A457, 2006, doi: 10.1149/1.2221767|issn 1099-0062.

[17] P. Svens, R. Eriksson, J. Hansson, M. Behm, T. Gustafsson, and G. Lindbergh, "Analysis of aging of commercial composite metal oxide – Li4Ti5O12 battery cells," *Journal of Power Sources,* vol. 270, no. 0, pp. 131-141, 12/15/ 2014, doi: http://dx.doi.org/10.1016/j.jpowsour.2014.07.050.

[18] C. Pastor-Fernández, K. Uddin, G. H. Chouchelamane, W. D. Widanage, and J. Marco, "A Comparison between Electrochemical Impedance Spectroscopy and Incremental Capacity-Differential Voltage as Li-ion Diagnostic Techniques to Identify and Quantify the Effects of Degradation Modes within Battery Management Systems," *Journal of Power Sources,* vol. 360, pp. 301-318, 2017/08/31/ 2017, doi: https://doi.org/10.1016/j.jpowsour.2017.03.042.

[19] B. Stiaszny, J. C. Ziegler, E. E. Krauß, M. Zhang, J. P. Schmidt, and E. Ivers-Tiffée, "Electrochemical characterization and post-mortem analysis of aged LiMn2O4–NMC/graphite lithium ion batteries part II: Calendar aging," *Journal of Power Sources,* vol. 258, pp. 61-75, 2014/07/15/ 2014, doi: https://doi.org/10.1016/j.jpowsour.2014.02.019.

[20] N. Yabuuchi and T. Ohzuku, "Novel lithium insertion material of LiCo1/3Ni1/3Mn1/3O2 for advanced lithium-ion batteries," *Journal of Power Sources,* vol. 119–121, no. 0, pp. 171-174, 6/1/ 2003, doi: http://dx.doi.org/10.1016/S0378-7753(03)00173-3.

[21] Q. Zhang and R. E. White, "Capacity fade analysis of a lithium ion cell," *Journal of Power Sources,* vol. 179, no. 2, pp. 793-798, 2008/05/01/ 2008, doi: https://doi.org/10.1016/j.jpowsour.2008.01.028.

[22] T. C. Bach *et al.*, "Nonlinear aging of cylindrical lithium-ion cells linked to heterogeneous compression," *Journal of Energy Storage,* vol. 5, pp. 212-223, 2016/02/01/ 2016, doi: https://doi.org/10.1016/j.est.2016.01.003.

[23] "3.7V 50Ah NCM Prismatic Li-Ion Battery Cell For EV." Osn Power. https://www.osnpower.com/3-7v-50ah-ncm-prismatic-li-ion-battery-cell-for-ev_p39.html (accessed June 11, 2021).